Off-line reaction monitoring of the oxidation of alkenes in water using drop coating deposition Raman (DCDR) spectroscopy

Abdolahzadeh, Shaghayegh; Boyle, Nicola M.; Draksharapu, Apparao; Dennis, Andrew C.; Hage, Ronald; de Boer, Johannes W.; Browne, Wesley R.

Published in:
Analyst

DOI:
10.1039/c3an00330b

Analyst

RSC Publishing

PAPER

View Article Online
View Journal | View Issue

Cite this: *Analyst*, 2013, **138**, 3163

Off-line reaction monitoring of the oxidation of alkenes in water using drop coating deposition Raman (DCDR) spectroscopy†

Shaghayegh Abdolahzadeh,[a] Nicola M. Boyle,[a] Apparao Draksharapu,[a] Andrew C. Dennis,[b] Ronald Hage,[c] Johannes W. de Boer[c] and Wesley R. Browne*[a]

Received 16th February 2013
Accepted 28th March 2013

DOI: 10.1039/c3an00330b

www.rsc.org/analyst

The application of drop coating deposition Raman (DCDR) spectroscopy to the field of reaction progress monitoring is addressed in this contribution. Although, DCDR spectroscopy has seen recent application in the study of biological fluids, its application in other areas has not yet been explored. Here we apply the technique to the catalysed oxidation of alkenes to epoxides in aqueous solutions at concentrations <10 mM. The effect of surface characteristics, background interferences, homogeneity of distribution of analytes, drying time, as well as instrumental limits of detection and calibration are discussed. We demonstrate that reproducible spectra can be obtained routinely, with relatively little variance, with short acquisition times and samples volumes of 2–10 μl and as little as 1 μg of analyte. The utility of the technique compared with online reaction monitoring by ^{1}H NMR and Raman spectroscopy is demonstrated in the excellent correlation between data obtained off and on-line.

Introduction

Over the last decades Raman spectroscopy[1] has proven to be a versatile and cost effective analytical method in all fields of chemical sciences for qualitative and quantitative chemical analysis, in particular for multi-component samples.[2] The technique has developed rapidly over the last decade due to the decrease in the cost of lasers and detectors and the increase in detector sensitivity. More importantly, the relatively weak Raman scattering cross-section of water and the spectrally rich 'chemical fingerprint' presented by compounds and materials allows for analysis of mixtures as complex as whole cells. Further advantages presented by Raman spectroscopy are the absence of or only minimal sample preparation required, non-destructiveness and rapidity of both on- and off-line analyses.[3] These characteristics have led to the extensive application of Raman spectroscopy for reaction monitoring and, in particular in industrial settings, for process control.[4]

The inherent weakness of the Raman scattering, however, means that species present at low concentration are difficult to detect both qualitatively and quantitatively (*e.g.*, <0.1 to 50 mM; the actual concentration limit being dependent both on the analyte in question and the system *S*/*N* characteristics). Several approaches can be taken to overcome this, including enhancement either by excitation at a wavelength resonant with an analytes electronic absorption band, *i.e.* resonance Raman (RR) spectroscopy,[5] surface enhanced Raman spectroscopy (SERS)[6] or a combination of both, *i.e.* surface enhanced resonance Raman spectroscopy (SERRS).[7] Although RR, SERS and SERRS are powerful methods to obtain valuable structural and electronic information, they are not universally applicable methods and often require the use of non-standard excitation wavelengths and roughened metal surfaces or nanoparticles exhibiting surface plasmon bands at the appropriate wavelength.

Recently, an alternative approach has been taken by several groups in the *drop coating deposition Raman* (DCDR) method.[8] The DCDR method takes a relatively simple approach to overcoming the detection limit of Raman spectroscopy, by pre-concentration of dilute solutions (*i.e.* solvent removal) prior to analysis. The technique is based on the well-known coffee stain effect;[9,10] when a microdroplet is applied to a surface under certain conditions, the majority of nonvolatile materials concentrate at the edge of an evaporating droplet,[8,9,11] thereby allowing for an increase by several orders of magnitude in the mass of the analyte present in the volume sampled by a Raman microspectrometer. The DCDR method has been applied recently in the analysis of biomaterials including human, bovine, and porcine insulin,[12] lysozyme,[13] glucose, glycan, taxane,[14] domoic acid,[15] human tear fluid[16] and the synovial fluid of osteoarthritis patients, among other biomaterials that are present in serum at low concentrations.[17] An important feature

[a]*Stratingh Institute for Chemistry, Faculty of Mathematics and Natural Sciences, University of Groningen, Nijenborgh 4, 9747AG, Groningen, The Netherlands. E-mail: w.r.browne@rug.nl; Tel: +31 50363 4428*

[b]*Andor Technology, Millenium Way, Belfast, Northern Ireland*

[c]*Catexel BV, BioPartner Center Leiden, Galileiweg 8, 2333 BD Leiden, The Netherlands*

† Electronic supplementary information (ESI) available: Details of synthesis and additional spectral data. See DOI: 10.1039/c3an00330b

of the DCDR method was demonstrated by Zhang *et al.* in the segregation of proteins and salts during the drying process, which further enhances the signal strength achievable in complex biological matrices.[12,14]

Although increasingly applied in the qualitative and sometimes quantitative analysis of biological serums and fluids, the DCDR method presents potential opportunities in the analysis of synthetic and catalytic reaction mixtures also. This is especially the case for reactions carried out in water where the solubility of substrates is generally poor and in high-throughput screening of, *e.g.*, enzymatically, catalyzed reactions where the volume and mass of analyte available are often limited. Furthermore, when substrates are soluble in water, and especially when they do not bear chromophoric moieties, their polarity often presents problems in analysis with other techniques such as HPLC or GC.

In the present contribution, we explore the potential, to the best of our knowledge for the first time, of the DCDR technique to monitor reaction progress. As a test case we examine the catalytic epoxidation of alkenes by manganese catalysts in water quantitatively and qualitatively. This class of functional group transformation is especially suited for analysis by Raman spectroscopy since scattering from the alkene stretching mode is relatively intense as are the ring breathing modes of the epoxide product. Here we show that the DCDR method is suitable for such analysis and we address issues including the effect of surface characteristics, background interferents, homogeneity of distribution of analytes as well as instrumental limits of detection and calibration. We demonstrate the utility of the technique in reaction monitoring by direct comparison with online monitoring by ^{1}H NMR and Raman spectroscopy.

Experimental

Synthesis

4-Vinyl benzoic acid (**VBA**), 4-(oxiran-2-yl)benzoic acid (**OBA**), and styrene sulfonate sodium salt [**SS**, ^{1}H NMR (D_2O, 400 MHz): 7.79 (2H, d, 9 Hz), 7.62 (1H, d, 9 Hz), 6.85 (2H, dd, 11 Hz and 17 Hz), 5.95 (1H, dd 1 Hz and 17 Hz), 5.43 (1H, dd 1 Hz and 11 Hz) ppm] were obtained from Sigma-Aldrich (Steinheim, Germany). Commercially available chemicals were used without further purification unless stated otherwise. H_2O_2 was 50% w/w in water (Acros Organics). $[Mn_2O_3(tmtacn)_2](PF_6)_2\cdot H_2O$ (**1**) and $[Mn_2(O)(OAc)_2(tmtacn)_2](PF_6)_2$ (**2**) where tmtacn is *N*,*N*′,*N*″-trimethyl-1,4,7-triazacyclononane (Fig. 1), were available from earlier studies.[18]

Caution: The drying or concentration of solutions that potentially contain H_2O_2 should be avoided. Prior to drying or concentrating, the presence of H_2O_2 should be tested for using peroxide test strips followed by neutralization on solid $NaHSO_3$ or another suitable reducing agent. When working with H_2O_2, suitable protective safeguards should be in place at all times.

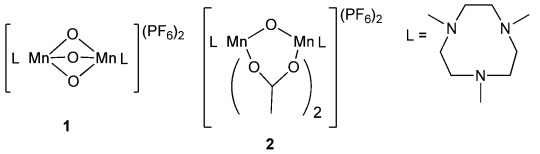

Fig. 1 $[Mn_2O_3(tmtacn)_2](PF_6)_2\cdot H_2O$ (**1**), $[Mn_2O(OAc)_2(tmtacn)_2](PF_6)_2$ (**2**) and the ligand, tmtacn.

Preparation of 4-(oxiran-2-yl)benzoic acid (OBA) from VBA

$[Mn_2O_3(tmtacn)_2](PF_6)_2\cdot H_2O$ (**1**, 0.8 mg, 1.0 μmol)[19] in 1 mL of water was added to 4-vinylbenzoic acid (148 mg, 1 mmol) in 100 mL of $NaHCO_3$(aq.) (0.1 M) followed by addition of H_2O_2 (50% in water, 283 μL, 5 mmol, 5 equiv. w.r.t. **VBA**) with stirring. The reaction mixture was stirred overnight. After the H_2O_2 had been consumed, the solution was acidified to pH 3 with dilute HCl and extracted into CH_2Cl_2. The organic layer was dried over Na_2SO_4 (anhydr.) and the solvent removed *in vacuo*. Elem. anal. found (calculated) C 65.7 (65.85)%, H 4.94 (4.91)%.

Preparation of 4-oxirane-phenyl-sulfonate (OS) from SS

The epoxide formed from the sodium salt of styrene sulfonate (**SS**) was prepared using a procedure adapted from that described earlier by de Boer *et al.*[18b] (see ESI also†). H_2O_2 (50% w/w, 7 μL) was added to a solution of **1** (2.0 mg, 2.5 μmol) and salicylic acid (3.5 mg, 25 μmol) in acetonitrile (1 mL) at room temperature. The mixture was stirred for 20 min after which 0.4 mL was added to **VS** (206 mg, 1 mmol) in water–acetonitrile (6 mL, 7 : 3, v/v). The mixture was cooled to 0 °C and H_2O_2 (50% in water, 63 μL, 1.1 mmol, 1.1 equiv. w.r.t. substrate) was added *via* syringe pump at a rate of 7.8 μL h^{-1}. The mixture was stirred and allowed to the reach room temperature over 16 h. ^{1}H NMR analysis of a 1 mL aliquot indicated approximately 50% conversion of **SS**. A second portion of freshly prepared catalyst containing solution and a second portion of peroxide was added (by syringe pump) and stirring continued for a further 14 h. The solvent was removed by lyophilisation and the product was purified by flash precipitation into acetonitrile, yielding the product 4-oxirane-phenyl-sulfonate, 130 mg, 0.59 mmol, 59%. ^{1}H NMR (D_2O, 400 MHz): 7.82 (2H, d, $J = 16$ Hz), 7.49 (2H, d, $J = 16$ Hz), 4.14 (1H, t, 4 Hz), 3.32 (1H, t, 4 Hz), 3.08 (1H, dd 3 Hz and 4 Hz) ppm.

Preparation of 4-(1,2-dihydroxyethyl)phenylsulfonate sodium salt (DS) from SS

The diol (**DS**) formed from styrene sulfonate (**SS**) was synthesised according to a method described by Lam *et al.*[20] A mixture of styrene sulfonate (340 mg, 1.65 mmol) and *m*CPBA (415 mg, 2.40 mmol) were dissolved in water–ethanol (40 mL, 1 : 1, v/v). The mixture was stirred for 2 h at 65 °C at which point all oxidant had been consumed (determined by testing with bromine water). The solution was allowed to cool and the solvent was removed *in vacuo*. Residual *m*-chlorobenzoic acid was dissolved in acetone (300 mL) and the remaining white product was isolated by filtration, dissolved in water and purified by flash precipitation into acetonitrile, yielding the product; 378 mg, 1.57 mmol, 95%. ^{1}H NMR (D_2O, 400 MHz): 7.83 (2H, d, $J = 9$ Hz), 7.56 (2H, d, $J = 9$ Hz), 4.89 (1H, t, $J = 5.5$ Hz), 3.79 (1H, m) ppm.

Instrumentation

^{1}H NMR (400.0 MHz) and ^{13}C NMR (100.6 MHz) spectra were recorded on a Varian Avance400. Chemical shifts are relative to DOH (4.79 ppm). Contact angles were measured on a Device Dataphysics instrument with SCA20, software version 3.60.2. A 2 μL drop of doubly distilled deionized water was used as the measuring liquid (sessile drop method). A minimum of five spots on each sample were probed and the contact angles averaged. Analysis consisted of applying a baseline and elliptical curve fitting of the water–air contact profile. The uncertainty in the measurements is (±3°).

Raman spectra were recorded using a Raman microscope (Perkin Elmer Raman station with an Olympus BX-51 microscope and long working distance objectives) at 785 nm (typically 20 mW at sample with a 50× long working distance objective) at room temperature. Raman spectra were recorded typically with 10 exposures of 8 s duration. Raman spectra at 532 nm were recorded using a homebuilt system consisting of an Andor Technology iDus-420-OE CCD camera, a Shamrock163 spectrograph and a 532 nm (300 mW, Cobolt) laser, both fibre coupled to an Inphotonics 532 nm Raman probe. Raman spectra were recorded typically with 20 exposures of 2 s duration. Reactions were carried out in a quartz 3 cm^3 volume 1 cm path length cuvette during on-line monitoring.

Catalyzed oxidation of VBA and SS

Oxidations of **VBA** and **SS** with H_2O_2 (50% w/w in water), catalysed by **1** or **2**, were carried out in 50 mL round bottomed flasks at 20 °C. pH was adjusted prior to addition of oxidant using with H_2SO_4(aq.) or NaOH(aq.) to pH 8.5.

Preparation of surfaces

Prior to modification, quartz slides were rinsed in turn with 10% hydrochloric acid, water, acetone and then ethanol. The slides were subjected to air plasma cleaning (Diener electronic, Femto) at 100 W, for 1 min (at 1.7 × 10^{-1} mbar air). Quartz slides were functionalized with a 4 mM solution of 1*H*,1*H*,2*H*,2*H*-perfluorooctyltriethoxysilane or octyltriethoxysilane in toluene with heating at reflux overnight. After functionalization, the surface was rinsed with ethanol followed by dichloromethane and dried under a nitrogen gas stream at r.t.

Analysis of Raman spectra obtained using DCDR

Spectra obtained following DCDR were analyzed in the spectral range 1800 to 600 cm^{-1}. The inconsistencies in the contribution of the carbonate buffer both spectrally and in terms of intensity precluded the reliable use of chemometric analysis and instead a manual data reduction and fitting approach using Microsoft Excel™ was taken. Spectra of the main reaction components, *i.e.* the alkene, epoxide and diol, were recorded by DCDR from carbonate buffered solutions at the pH used under reaction conditions. Fitting of a weighted sum of the substrate and product spectra provided the mole fraction of each component in a mixture.

The data analysis began with an offset correction followed by normalization of the spectra to the area of the bands between 1600 and 1650 cm^{-1}, which includes contributions from the reactant and products only. The raw spectra of mixtures of alkene and epoxide were then fitted with a weighted sum of the spectra of the pure components and an offset correction to provide the mole fraction of substrate and product in the mixture. Spectral fitting involved minimization of the bands of the substrate and product in the residual spectra (*i.e.* real spectrum – calculated spectrum) in spectral regions where the carbonate or other components do not show signals. A calibration curve was constructed with mole fraction increments of 0.05 for both **VBA** and **SS**. The advantage of this approach to the analysis lies in the absence of a need to apply a baseline correction and the effect of spectrum to spectrum variations in absolute intensity and background signals.

Results

Model reactions

In the present study, the catalysts $[Mn_2O_3(tmtacn)_2](PF_6)_2\cdot H_2O$ (**1**) and $[Mn_2O(OAc)_2(tmtacn)_2](PF_6)_2$ (**2**), where tmtacn is *N*,*N*′,*N*″-trimethyl-1,4,7-triazacyclononane (Fig. 1), were employed in the epoxidation of water soluble alkenes with H_2O_2.

Catalyst **1** was identified as a highly effective catalyst for low temperature bleaching of clothing and for the epoxidation of styrene in water in the 1990s[21] and was later applied in a wide range of oxidative functional group transformations in organic solvents.[22] Currently our group is investigating the application of these catalysts in aqueous media for alkene oxidation. For many substrates the relatively low solubility of the substrate and/or products in aqueous media has posed a considerable challenge in terms of analysis, both on- and off-line, especially in large scale reaction conditions and in high-throughput screening programs. This prompted us to investigate the possibility of applying the DCDR method for both the analysis of overall conversion and also in obtaining kinetic data for reactions where the reaction times are >1 h.

We examined the oxidation of two model substrates (Scheme 1); *i.e.* 4-vinylbenzoic acid (**VBA**) and styrene-*p*-sulfonate (**SS**) in water with H_2O_2 catalyzed by **1**.

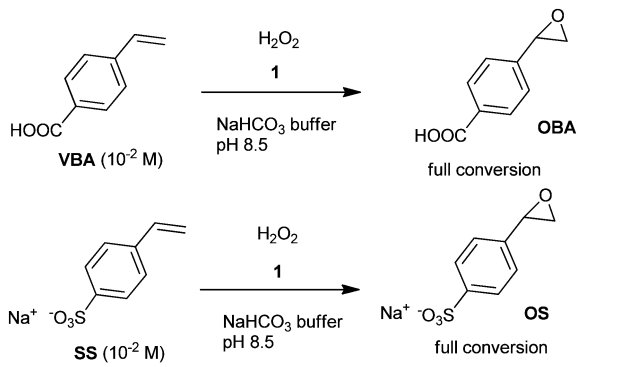

Scheme 1 Model reactions examined; the oxidation of 4-vinylbenzoic acid (**VBA**) and styrene-*p*-sulfonate (**SS**).

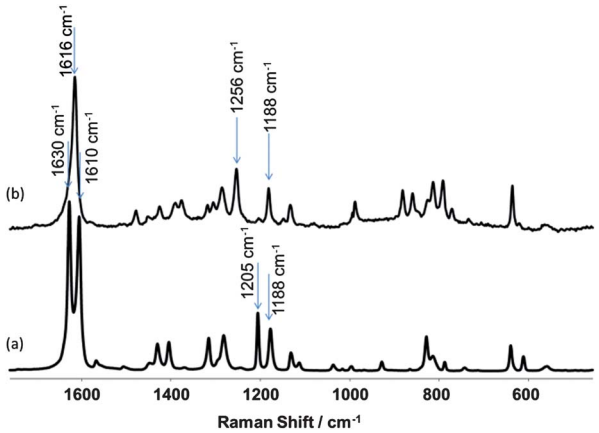

Fig. 2 Solid state Raman spectra (λ_{exc} 785 nm) of (a) **VBA** and (b) its epoxide product **OBA**. Bands of most interest with respect to analysis are indicated.

Reactions were carried out in a total volume of 3 mL of aqueous $NaHCO_3$ (10^{-1} M). Typical concentrations employed were 10 mM substrate, 10 μM catalyst and 50 mM H_2O_2. In the case of **VBA**, the substrate dissolved in the carbonate buffer only upon addition of H_2O_2 and hence time zero is taken to be the point at which the catalyst is added. Unless stated otherwise all reactions were performed at ambient temperature (20–23 °C).

Solid state Raman spectroscopy

Raman spectra of **VBA** and its epoxide product (**OBA**) are shown in Fig. 2 and those of **SS** and **OS** in Fig. 3. Of particular interest with regard to analysis are the differences between the spectra in the ranges 1200–1300 cm^{-1} and 1600–1650 cm^{-1} and to a lesser extent the range between 600 and 900 cm^{-1}, as these regions do not suffer interference from Raman scattering from carbonates (*vide infra*). The bands in the range 1600–1650 cm^{-1} are characteristic of C=C stretching vibrations of vinyl and aryl groups and in particular the band at 1630 cm^{-1} is useful in monitoring reaction progress.

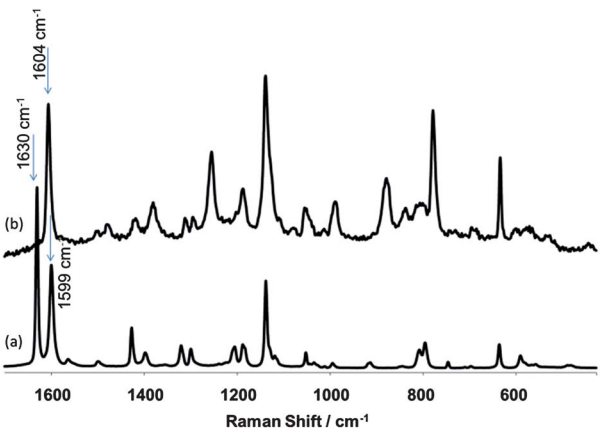

Fig. 3 Solid state Raman spectra (λ_{exc} 785 nm) of (a) **SS** and (b) its epoxide product **OS**. Bands of most interest with respect to analysis are indicated.

Effect of surface pretreatment on drying pattern and Raman analysis

A range of surfaces for DCDR studies have been employed previously by several groups, including quartz,[12,23,24] calcium fluoride,[13] coated or uncoated glass, PTFE coated stainless steel, and gold foil.[8] The primary consideration in the choice of surface is that it is chemically inert with regard to the analyte and solution, presents little or no background signal and has a low optical absorbance to limit sample heating during measurements. Quartz slides are readily available and were chosen to avoid the fluorescence at λ_{exc} 785 nm observed with borosilicate glass. The pattern formed by non-volatile reaction components upon drying depends on the characteristics of the surface used. Hence plasma treated quartz slides were compared with slides that were subsequently silanised with alkyl or perfluoroalkyl silanes.

Droplets of 10 mM solutions of the analytes (2 μL) were allowed to dry on quartz slides to achieve solute deposition in patterns that were found to be dependent on the type of surface treatment employed. Evaporation was accelerated by applying a low vacuum (10–20 mm Hg). The deposited analytes were observed by optical microscopy and in all cases the deposition was in the shape of a ring (coffee stain pattern) with some material deposited in the centre of the ring (Fig. 4). Although the shape of the deposition on the more hydrophobic surface is less uniform, the majority of the analyte was deposited on the outermost edge of the ring, whereas on the hydrophilic surface the analyte is more thinly deposited in a series of thin rings. An additional factor affecting deposition is ionic strength. In the case of the more water soluble **SS**, deposition from aqueous solutions did not show the desired coffee stain pattern except when the ionic strength was increased by addition of $NaHCO_3$ or NaCl.

In general it can be concluded that uniform 'coffee stain patterns' cannot be assumed for a particular system and care should be taken to study not only the drying patterns under ideal conditions but also the effect of side reactions and additional reaction components.[25] For example, the irregular shape of the residue deposited upon drying of the droplet indicates that the droplet is not pinned during the drying process.

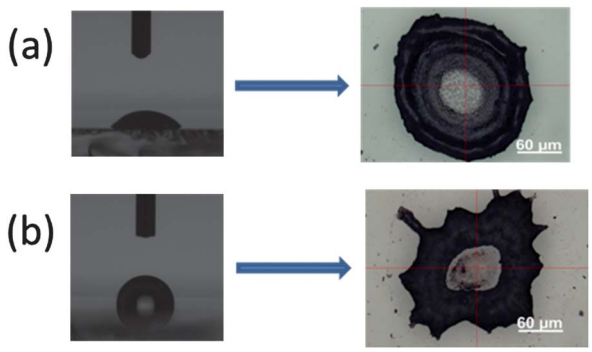

Fig. 4 Dependence of the drying pattern (2 μL of a 10 mM solution of **VBA** in 0.1 M $NaHCO_3$ (aq.), pH 8.5, mass of analyte *ca.* 3 μg) on surface pre-treatment (a) plasma cleaned surface (contact angle 41°) and (b) plasma cleaned surface followed by silanisation with alkyl silanes (contact angle 103°).

Raman spectra of compounds deposited on hydrophobic surfaces

Solutions of **VBA** and **OBA** in $NaHCO_3$ buffer were deposited on hydrophobic quartz surfaces and Raman spectra were recorded at the edges of the depositions (Fig. 5). The Raman confocal volume (with a 50× objective) has a waist of approximately 5–10 microns[26] while the diameter of the deposition is approximately 250–300 microns and the width of the ring is 40 microns (see Fig. 4).

The DCDR analysis method relies on uniform co-deposition of the reaction components. Hence it is essential to verify the uniformity or otherwise of the distribution of various components across the deposition and the reproducibility of spectra both at the same point, at different points on a particular deposition and over several depositions. The distribution was investigated using solutions of a range of mole fractions of **VBA** and **OBA**. Three depositions were made at each of the three different mole fractions, followed by recording Raman spectra at eight points across each of the nine depositions (Fig. 6). Each sample point was recorded using a 100× objective and the laser spot size and therefore waist of the confocal volume was <5 microns. Visual inspection of the dried spots of **VBA**, **OBA** and mixtures of both indicates that most of the material deposits in a 30–40 micron wide ring with a diameter of 250 microns, which is confirmed by comparison of Raman spectra recorded at the edge of the spot (*i.e.* points a–f) and at the centre (*i.e.* points g and h); the latter spectra being essentially featureless.

As expected, the absolute intensity of the individual spectra is highly variable due to the lack of uniformity in terms of thickness of the deposited material in the deposition. Nevertheless, after normalisation (to the maximum in the 1600–1650 cm^{-1} region where carbonates do not contribute), the standard deviation of the Raman spectra recorded at various points around the ring of each sample and between several spots for three mole fraction mixtures (0.2, 0.6 and 0.8) was found to be *ca.* 2–3%, which indicates that the distribution can be treated as uniform for the two components **VBA** and **OBA**. By contrast, the distribution with respect to carbonates was not uniform as can be seen from the comparison of the average

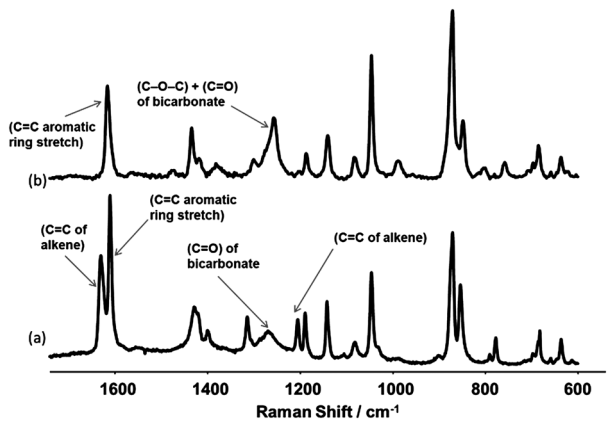

Fig. 5 Raman spectra (λ_{exc} 785 nm) of (a) **VBA** and (b) **OBA** obtained on a treated hydrophobic surface. Regions of most interest are noted.

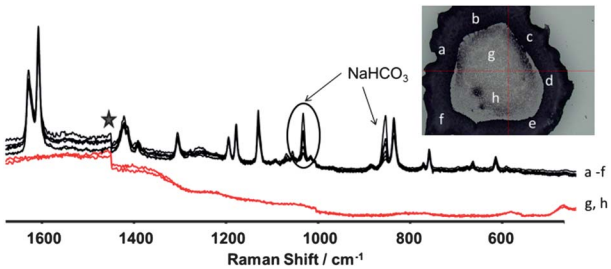

Fig. 6 Raman spectra (λ_{exc} 785 nm) recorded at eight points across a deposit. The spectra are overlaid in the lower panel and demonstrate the spectral consistency at multiple points on the outer ring except for contributions (both shape and intensity) from the carbonate buffer. The star indicates a spectral artefact.

spectrum and the standard deviation at each wavenumber (see ESI Fig. S5†). Furthermore, the contributions of the various carbonate species to the spectra were found to be highly variable over the entire deposition.

The ratio of the two components (**VBA** and **OBA**) was calculated by fitting the average spectra with a model, based on spectra obtained using DCDR from (carbonate free) aqueous solutions of **VBA** and **OBA**. The spectra were processed by offset correction and normalization. Each spectrum was then fitted with a model to obtain the best fit in the region between (1600–1650 cm^{-1}), which is dominated by the alkene and vinyl C=C stretching modes and the 1100–1200 cm^{-1} region. These regions were selected since the variability in other regions (*e.g.*, between 1000 and 1100 cm^{-1}) precluded their use in fitting, due to the presence of varying contributions from carbonates. Fitting of the average spectra at 20 mol%, 60 mol% and 80 mol % of **OBA** w.r.t **VBA** shows a good correlation with the expected values, which indicated that a calibration curve can be prepared in this manner (*vide infra*).

Quantitative analysis

A calibration curve for **VBA**/**OBA** was prepared by the method of continuous variation holding the total concentration to that employed in the catalysed oxidation reactions (10 mM, *vide infra*). Samples were deposited on a hydrophobic surface (see Experimental section) and Raman spectra were obtained at λ_{exc} 785 nm. Fitting provided good agreement with the expected values, albeit close to the extremes (<0.2 and >0.8) the accuracy decreases as the limits to detection of one of the components are approached (Fig. 7).

The detection limits in Raman spectroscopy are highly dependent on the power of the excitation laser, the efficiency of the light collection optics and the characteristics of the detector employed. Nevertheless it is informative to consider the effect of initial sample volume (2–10 μL) and concentration of the analyte, **VBA** (0.1 mM to 10 mM), on the limits of detection in the presence of 0.1 M $NaHCO_3$ buffer (Fig. S5†). Depositing 10 μL of a 0.5 mM solution of **VBA** (*i.e.* 740 ng of substrate) still allowed for detection above the noise. The dependence of the final spot size after drying on the sample volume is shown in Fig. 8. In general, a larger spot diameter is obtained with increased

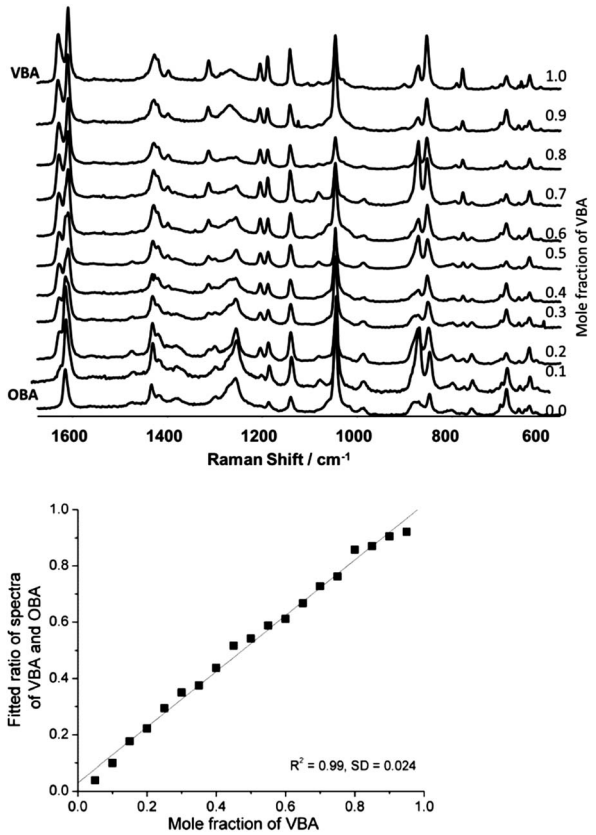

Fig. 7 Raman spectra obtained from various mixtures of **VBA** and **OBA** (2 μL droplets, the total concentration, *i.e.* [**VBA**] + [**OBA**] was held at 10 mM) in $NaHCO_3$ (0.1 M) buffer and the calibration curve obtained. The uncertainties due to fitting are estimated to be ±<5%.

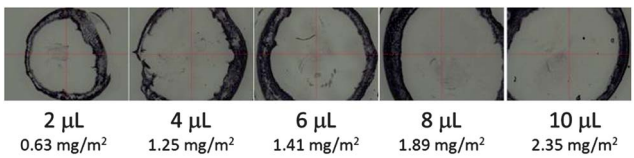

Fig. 8 Images of deposits formed using different volumes of solution containing 0.5 mM **VBA** and 0.1 M $NaHCO_3$. The density of material in the areas where **VBA** is deposited in the ring indicated in mg m^{-2} was estimated geometrically. The dimensions of the area imaged in each case are 200 μm by 155 μm.

sample volume; however, the width of the outer ring, in which the components of interest are concentrated, is relatively unaffected. Hence, by increasing the volume of analyte sampled the absolute intensity of the Raman spectrum obtained and hence the signal to noise ratio can be increased, albeit at the cost of requiring larger sample volumes.

Distribution of compounds of differing solubility

The DCDR analysis method relies on the uniform co-deposition of reaction components of interest with respect to the sampled volume. Precipitation of compounds occurs upon evaporation of water from the droplet and although the polarity **VBA** and **OBA** are similar, this is not necessarily the case for other reaction products such as the analogous diol product or benzaldehyde. The differences in solubility that can be tolerated by the technique was explored by DCDR analysis of mixtures of **VBA** and **SS**, the latter showing orders of magnitude higher solubility in the applied media than the former (Fig. 9). As above, the spectra were analysed using spectra obtained from DCDR of solutions containing only **VBA** or **SS** to determine the mole fraction of each component, which was plotted against the calculated mole fraction. A reasonably good distribution about the best fit was obtained and importantly, the spectra obtained from different points in individual deposits and for different deposits obtained from the same mixture were uniform in the ratio of the spectral contribution of each of the two components (see Fig. S6 to S11†).

Reaction progress monitoring by DCDR spectroscopy

The time taken for the solvent (*i.e.* H_2O) to evaporate and for the deposit to form is, potentially, a limiting factor in the time resolution that can be achieved using the DCDR method. This limitation is reduced to a certain extent by the use of vacuum to accelerate evaporation (from *ca.* 20 min under ambient conditions to *ca.* 5 min). For reactions that proceed over relatively long periods (*i.e.* >1 h) direct online analysis of large numbers of reactions is relatively expensive in terms of the resources required. With the DCDR method, however, analysis can be carried out in batch fashion assuming, of course, that the reaction stops upon drying.

The effect of drying rate on the analysis was examined by comparison of two samples deposited simultaneously but with one dried under ambient conditions (evaporation time *ca*. 20 min) and the second dried *in vacuo* (evaporation time <5 min). From the spectra shown in Fig. 10, it is apparent that for the sample dried under ambient conditions the reaction progressed further (38%) than for the sample dried *in vacuo* (20%); note the differences in the band structure at *ca.* 1610 cm^{-1}. These

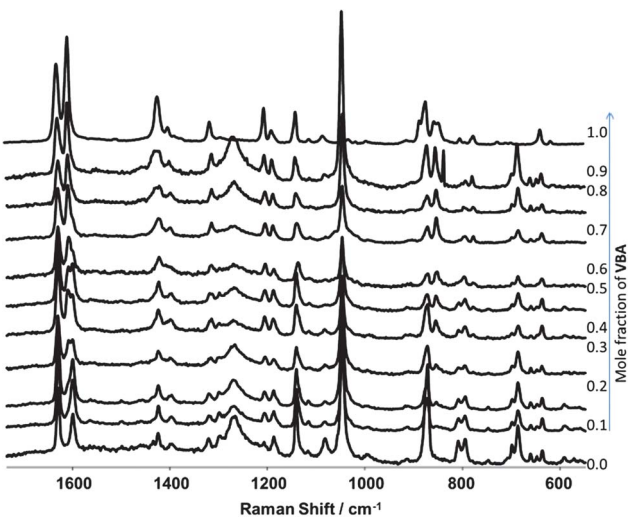

Fig. 9 Raman spectra obtained from various mixtures of **VBA** and **SS** drying 2 μL of 10 mM (total concentration) solutions in 0.1 M carbonate buffer (sample mass *ca*. 3 μg).

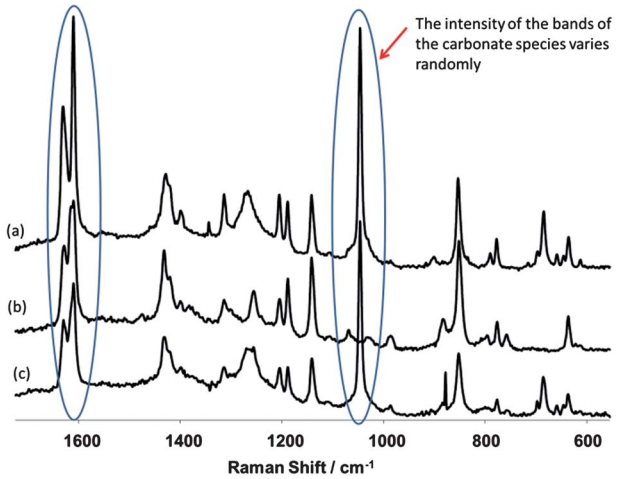

Fig. 10 Comparison of spectra obtained from (a) a reaction mixture form which the catalyst was omitted, a reaction mixture with catalyst present with the droplet sample dried (b) under ambient conditions and (c) dried *in vacuo*.

differences can be understood by considering that the concentration of reactants increases upon drying and hence reaction rate should increase; however, the increase is counterbalanced to some extent by the simultaneous deposition of substrate and product that occurs.

Comparison of on-line *vs.* off-line (DCDR) methods

The utility of the DCDR method for off-line reaction progress monitoring was assessed by direct comparison with on-line reaction monitoring by both Raman and ^{1}H NMR spectroscopy. In Fig. 11, conversion calculated by the DCDR method and on-line reaction monitoring by Raman spectroscopy, show good agreement and indeed both techniques allowed for the observation of changes in reaction rates overtime (the induction period is due to minor changes in pH as the reaction proceeds). A discrepancy (*ca.* <3%) in the conversion determined by both methods is ascribed to additional conversion which takes place during droplet drying (*vide supra*).

Comparison of reaction progress monitored by the DCDR method and by *in situ* ^{1}H NMR spectroscopy, highlighted an important point in regard to obtaining kinetic information by direct measurement. Immediately after addition of H_2O_2 to the reaction mixture a sample was withdrawn for on-line ^{1}H NMR analysis, with spectral acquisition at intervals equal to the rate of sampling of the reaction mixture by DCDR. The reaction progress determined from the sample held in the NMR spectrometer showed a significant discrepancy to that determined by DCDR. The origin of the discrepancy was identified by taking a second sample from the reaction mixture for ^{1}H NMR analysis at the end of the monitoring period, which showed that conversion in the NMR tube used for online analysis was different to that obtained in the bulk reaction mixture from which DCDR analysis was performed. Sampling of the reaction mixture at set intervals for analysis by both techniques was therefore performed to avoid this problem. Comparison of the conversion determined by both methods shows good agreement over the entire course of the reaction (Fig. 12).

Use of DCDR in high-throughput screening of reaction conditions

The application of DCDR for reaction progress monitoring is demonstrated in the oxidation of **VBA** to **OBA** and in the oxidation of **SS** to **OS** with H_2O_2 catalysed by **1** or **2**. The reaction rate

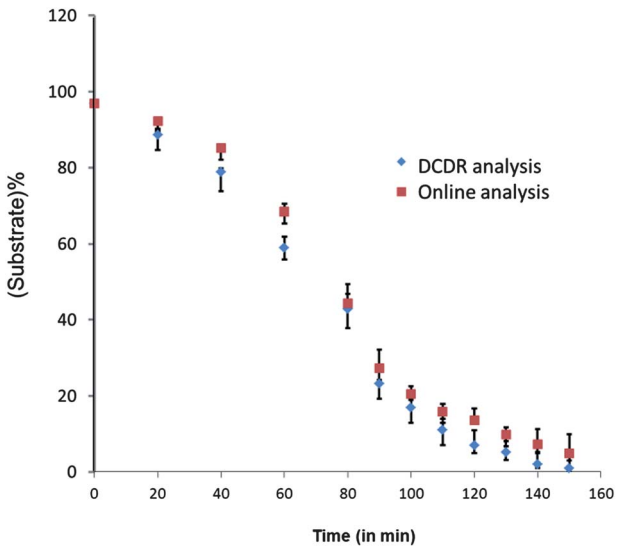

Fig. 11 On-line reaction monitoring at 532 nm (ref. 27) (solid squares) overlaid with results from off-line analysis with DCDR (open circles) of the same reaction mixture. *Reaction conditions*: **VBA** (10 mM), H_2O_2 (50 mM), $NaHCO_3$ (0.1 M). t = 0 is the point at which the catalyst (**2**, 2 μM) was added. Raman spectra were acquired on-line with 4 min intervals. Samples for off-line analysis were taken at indicated time points, drying times were <4 min.

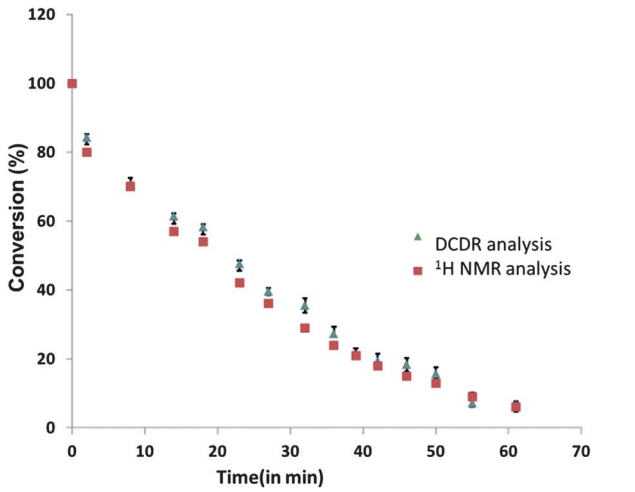

Fig. 12 Off-line monitoring of reaction progress in the oxidation of **VBA** (0.01 M) with H_2O_2 (0.05 M) catalysed by **2** (10 μM) in $NaHCO_3$(aq.) (0.1 M) in D_2O (the **VBA** was solubilised by addition of H_2O_2 prior to addition of **2**). 700 μL and 2 μL aliquots were removed at the times indicated for analysis by ^{1}H NMR spectroscopy (with *tert*-butanol as internal standard) and DCDR spectroscopy, respectively. Analysis of the Raman spectra employed fitting with the spectra of **VBA** and **OBA** as described above.

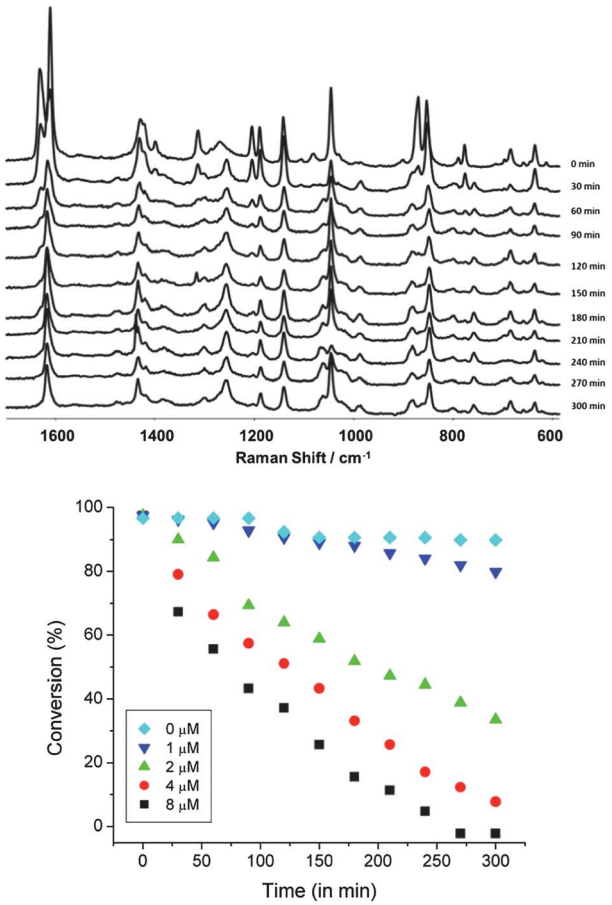

Fig. 13 (a) Raman spectra of a reaction mixture obtained at 30 min time intervals at 8 μM of **2**. (b) Substrate conversion with time for catalyst **2** concentrations between 0 and 8 μM. The reactions were performed in parallel and spectral acquisition for the entire DCDR sample set was carried out in approximately 1 h.

shows a dependence on catalyst concentration. The intensity of the Raman band at 1631 cm^{-1} can be seen to decrease as the reaction progresses where 8 μM of **1** was used. Fitting the spectra obtained by DCDR as described above allows for determination of the mole fraction of **VBA** at each time point. At lower catalyst concentrations the reaction rate decreases. The data obtained by the DCDR method for five reactions in parallel (55 data points in total) is shown in Fig. 13. The data indicate that the reaction is non-linearly dependent on catalyst concentration.

Conclusions

Previous studies have shown that inhomogeneous deposition can be a problem in DCDR for large molecules such as proteins.[16,21] For smaller molecules, our results confirm that drop coating deposition of compounds of substantially differing solubility show essentially homogeneous deposition.[26] The spectra obtained in this study using the DCDR technique are reproducible with relatively little variance (<2%) and can be obtained with short acquisition times and small samples volumes. The time taken for the solvent (*i.e.* H_2O) to evaporate and the deposit to form is a potentially limiting factor in the time resolution that can be achieved using the DCDR method. However, for reactions that proceed over relatively long periods (*i.e.* >1 h) off-line analysis of large numbers of reactions by the DCDR method offers a relatively inexpensive approach both in terms of facilities required and time, in comparison with commonly employed techniques such as GC and HPLC or online monitoring. A key advantage in the catalytic reaction studied in the present report in comparison with on-line Raman or off line ^{1}H NMR spectroscopy is that rapid drying results in quenching of the reaction, which allows for analysis after the reaction at a later time and that much lower sample volumes are required.

The catalysed reactions studied here are highly suited to the DCDR technique. For other reactions control experiments must be made to ensure that the observations made here hold for those reactions also, especially with regard to homogenous deposition of reaction components over the sampled area. Nevertheless, in many cases we expect that this approach to reaction monitoring can be applied generally to reactions carried out under aqueous conditions. Extension of this method to non-aqueous conditions will be explored in future studies.

Acknowledgements

The authors thank the Netherlands Organisation for Scientific Research (VIDI Grant 700.57.428, WRB), the European Research Council (Starting Investigator Grant 279549, NMB, WRB), the University of Groningen (Ubbo Emmius studentship, AD), the Foundation for Technology and Science (STW Grant No. 11059, SA, NMB, JWdB, WRB) for financial support.

Notes and references

1 R. J. H. Clark, *Analyst*, 2013, **138**, 729.
2 *Raman Spectroscopy for Chemical Analysis*, ed. R. McCreery, John Wiley and Sons, New York, USA, 2005.
3 *Handbook of Raman Spectroscopy*, ed. I. R. Lewis and H. G. M. Edwards, Marcel Dekker, New York, 2001.
4 G. Févott, *Chem. Eng. Res. Des.*, 2007, **85**, 906.
5 (*a*) P. R. Carey, *Biochemical Applications of Raman and Resonance Raman Spectroscopies*, Academic Press, New York, 1982; (*b*) T. G. Spiro and C. A. Grygon, *J. Mol. Struct.*, 1998, **173**, 79; (*c*) T. G. Spiro and R. S. Czernuszewicz, *Methods Enzymol.*, 1995, **246**, 416; (*d*) J. C. Austin, T. Jordan and T. G. Spiro, *Adv. Spectrosc.*, 1993, **20**, 55.
6 (*a*) J. A. Dougan and K. Faulds, *Analyst*, 2012, **137**, 545; (*b*) I. R. Nabiev, K. V. Sokolov and M. Manfait, in *Biomolecular Spectroscopy*, ed. R. J. H. Clark and R. E. Hester, Wiley, Chichester, UK, 1993, ch. 7, vol. 21; (*c*) T. M. Cotton, J.-H. Kim and G. D. Chumanov, *J. Raman Spectrosc.*, 1991, **22**, 729; (*d*) T. M. Cotton, in *Spectroscopy of Surfaces*, ed. R. J. H. Clark and R. E. Hester, Wiley, New York, 1988, ch. 3.
7 T. M. Cotton, S. G. Schultz and R. P. Van Duyne, *J. Am. Chem. Soc.*, 1982, **104**, 6528.
8 D. Zhang, Y. Xie, M. F. Mrozek, C. Ortiz, V. J. Davisson and D. Ben-Amotz, *Anal. Chem.*, 2003, **75**, 5703.
9 R. D. Deegan, O. Bakajin, T. F. Dupont, G. Huber, S. R. Nagel and T. A. Witten, *Nature*, 1997, **389**, 827.

10 E. Kocisova, A. Vodakova and M. Prochazka, *Vibrational Spectr.*, 2006, **42**, 184.
11 D. Zhang, M. F. Mrozek, Y. Xie and D. Ben-Amotz, *Appl. Spectrosc.*, 2004, **58**, 929.
12 C. Ortiz, D. Zhang, Y. Xie, V. J. Davisson and D. Ben-Amotz, *Anal. Biochem.*, 2004, **332**, 245.
13 J. Filik and N. Stone, *Analyst*, 2007, **132**, 544.
14 P. Cipriani and D. Ben-Amotz, *J. Raman Spectrosc.*, 2005, **36**, 1052.
15 Y. Djaoued, S. Balaji and S. Priya, *Spectrochim. Acta, Part A*, 2007, **67**, 1362.
16 J. Filik and N. Stone, *J. Raman Spectrosc.*, 2009, **40**, 218.
17 K. A. Esmonde-White, G. S. Mandair, F. Raaii, J. A. Jacobson, B. S. Miller, A. G. Urquhart, B. J. Roessler and M. D. Morris, *J. Biomed. Opt.*, 2009, **14**, 034013.
18 (*a*) J. W. de Boer, W. R. Browne, J. Brinksma, P. L. Alsters, R. Hage and B. L. Feringa, *Inorg. Chem.*, 2007, **46**, 6353; (*b*) J. W. de Boer, J. Brinksma, W. R. Browne, A. Meetsma, P. L. Alsters, R. Hage and B. L. Feringa, *J. Am. Chem. Soc.*, 2005, **127**, 7990.
19 K. Wieghardt, U. Bossek, B. Nuber, J. Weiss, J. Bonvoisin, M. Corbella, S. E. Vitols and J. J. Girerd, *J. Am.Chem. Soc.*, 1988, **110**, 7398.
20 P. K. H. Lam, M. H. George and J. A. Barry, *Polymer*, 1989, **30**, 2320.
21 R. Hage, J. E. Iburg, J. Kerschner, J. H. Koek, E. L. M. Lempers, R. J. Martens, U. S. Racherla, S. W. Russell, T. Swarthoff, M. P. van Vliet, J. B. Warnaar, L. van der Wolf and B. Krijnen, *Nature*, 1994, **369**, 637.
22 G. De Faveri, G. Ilyashenko and M. Watkinson, *Chem. Soc. Rev.*, 2011, **40**, 1722; D. E. De Vos, B. F. Sels, M. Reynaers, Y. V. Subba Rao and P. A. Jacobs, *Tetrahedron Lett.*, 1998, **39**, 3221; A. Berkessel and C. A. Sklorz, *Tetrahedron Lett.*, 1999, **40**, 7965; J. Brinskma, L. Schmieder, G. van Vliet, R. Boaron, R. Hage, D. E. De Vos, P. L. Alsters and B. L. Feringa, *Tetrahedron Lett.*, 2002, **43**, 2619; J. W. de Boer, W. R. Browne, S. R. Harutyunyan, L. Bini, T. D. Tiemersma-Wegman, P. L. Alsters, R. Hage and B. L. Feringa, *Chem. Commun.*, 2008, 3747.
23 C. Ortiz, D. Zhang, Y. Xie, A. E. Ribbe and D. Ben-Amotz, *Anal. Biochem.*, 2006, **353**, 157.
24 R. A. Halvorson and P. J. Vikesland, *Environ. Sci. Technol.*, 2011, **45**, 5644.
25 R. D. Deegan, O. Bakajin, T. F. Dupont, G. Huber, S. R. Nagel and T. A. Witten, *Nature*, 1997, **389**, 827; T. Kajiya, E. Nishitani, T. Yamaue and M. Doi, *Phys. Rev. E: Stat., Nonlinear, Soft Matter Phys.*, 2006, **73**, 011601.
26 The spot size was found to be sufficiently large to still allow for acquisition of spectra representative of the bulk sample even where components crystallise separately.
27 A 532 nm Raman spectrometer was used for online monitoring as the 785 nm system used for analysis of the DCDR system was not sufficiently sensitive to provide a sufficient signal to noise ratio for reliable analysis (the laser power at sample was 200 mW at sample at 532 nm in contrast to 80 mW at sample at 785 nm). In addition the detector used has a higher sensitivity in the visible region than in the NIR.